JOURNAL OF MATERIALS SCIENCE 31 (1996) 4423–4431

High-performance aromatic polyimide fibres

Part V *Compressive properties of BPDA–DMB fibre*

WEIHAN LI, ZONGQUAN WU, HAO JIANG, M. EASHOO, F. W. HARRIS, S. Z. D. CHENG*
Maurice Morton Institute and Department of Polymer Science, The University of Akron, Akron OH 44325-3909, USA

A new polyimide has been synthesized from 3,3′,4,4′-biphenyltetracarboxylic dianhydride (BPDA) and 2,2′-dimethyl-4,4′-diaminobiphenyl (DMB). A high-strength, high-modulus, high-temperature fibre has been developed from this polyimide via a dry-jet wet spinning method. The tensile strength of BPDA–DMB fibres is 3.3 GPa and the tensile modulus is around 130 GPa. The compressive strength of the fibres has been investigated through a tensile recoil test (TRT), while the fibre morphology after compression has been studied via polarized light microscopy (PLM) and scanning electron microscopy (SEM). From the TRT measurements, we have observed that the compressive strength of this fibre is 665 (±5) MPa, which is higher than those of other aromatic polymer fibres. The effect of fibre diameter on the compressive strength of BPDA–DMB fibres is not substantial. The critical compressive strain for this fibre at which the kink bands start appearing under the observation of PLM is at 0.51–0.54%. Subglass relaxation processes have been observed and the measure of an apparent relaxation strength may serve as one of the factors which significantly affect the compressive strength of the fibres. Tensile tests of pre-compressed fibres reveal a continuous loss in tensile strength (up to 30%) with increasing the compressive strain (up to 2.6%). PLM and SEM observations show that during the compression BPDA–DMB fibres form regularly-spaced kink bands at ±60° (±2°) with respect to the fibre axis. The kink band density initially increases with the compressive strain, and reaches a maximum at around 1.1%. Further increase of the compressive strain decreases this density due to the merge of the neighbouring bands. The size of kink bands also correspondingly increases within this compressive strain region. The morphological observation via SEM implies the existence of a skin-core structure and microfibrillar texture which are common features in polymer fibres.

1. Introduction

High-performance polymeric fibres with high-strength, high-modulus and high-temperature properties have undergone a significant development in the last two decades. Polymer fibres have been prepared which show moduli higher than 350 GPa and tensile strength higher than 3.5 GPa [1]. However, the advantages in fibre tensile properties for structural composite applications are limited because these fibres have low axial compressive strength and this property often becomes the dominant factor in determining the ultimate composite properties [2, 3]. The compressive behaviour of fibres has been extensively studied over the past ten years. For many polymer fibres such as poly(*p*-phenylene benzobisoxyzole) (PBZO), poly(*p*-phenylene benzobisthiazole) (PBZT) and Kevlar fibres, the ratio of compressive strength to tensile strength varies between 5–10%. Table I lists some tensile and compressive properties of several high-performance fibres.

Recently, a new family of aromatic polyimide fibres based on 3,3′,4,4′-biphenyltetracarboxylic dianhydride (BPDA) have been developed in our laboratory [4–7]. The tensile properties of these fibres are similar or slightly superior to Kevlar fibres. One of the members in this family is the fibre spun via the polyimide synthesized from BPDA and 2,2′-dimethyl-4,4′-diaminobiphenyl (DMB) in *p*-chlorophenol. Its chemical structure is

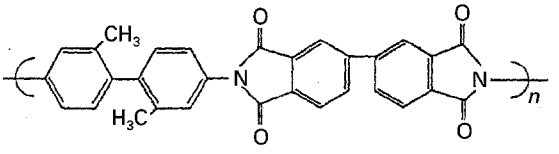

This BPDA–DMB fibre shows a tensile strength to break of 3.3 GPa and the tensile modulus of 130 GPa. The thermal and thermo-oxidative stability of this fibre is higher than that of Kevlar fibres [6]. These

*To whom all correspondence should be addressed.

0022–2461

TABLE I Tensile properties of high performance fibres

	BPDA–DMB	Kevlar-49	PBZO	C-fibre (T-40)
Density ($g\,cm^{-3}$)	1.35	1.44	1.58	1.81
Tensile strength (GPa)	3.3	3.5	3.7	5.6
Specific strength (GPa)	2.44	2.43	2.34	3.09
Tensile modulus (GPa)	130	124	360	289
Specific modulus (GPa)	96.3	86.1	228	160
Compressive strength (MPa)	665*	365	200	2756
Specific compressive strength (MPa)	493*	253	127	1523
Compressive strength/ tensile strength ratio	0.20*	0.10	0.05	0.49

*This data is reported in this work.

combined properties make the BPDA–DMB fibre a candidate for high-performance applications in structural materials and composites. The compressive strength of these BPDA–DMB fibres, which is one of the very important properties for the fibre applications, is not presently available. Obviously, investigating the compressive behaviour of BPDA–DMB fibres is necessary and may help to further explore and understand the compressive behaviour of uniaxially oriented polymer materials.

At present, a central problem is how to measure the compressive strength of polymer fibres. Most of the methods used are indirect measurements. For example, bending and elastic loop techniques have been employed to estimate fibre compressive strength [3, 8–11]. The compressive strength measured via these methods is, however, generally higher than that obtained in composites. The single filament embedded composite technique appears to provide better agreement [12], but often requires tedious procedures. It has been reported that the tensile recoil test (TRT) has been used to measure some high-performance polymer fibres and that the results are in good agreement with compressive strengths measured in fibre composite tests [13]. However, the results obtained using this method were critically associated with how to cut the fibres under tension. Direct methods include single filament compression using a micro-tensile testing machine [14] and a "nano-compressometer" [15]. In theory these methods should provide the most precise measurements without using the assumptions usually needed with indirect methods. Nevertheless, to obtain a buckling-free single filament in the measurements is often difficult due to the large ratio between the filament length and diameter.

In this paper, we report the axial compressive behaviour and morphology of BPDA–DMB polyimide fibres. The TRT method was utilized by rupturing the filament with an electric spark [16]. It has been found that better control of the failure stress and hence reproducible results can be achieved by using a very slow tensile strain rate.

2. Experimental procedure

2.1. Materials and fibre spinning

The polymer was prepared by the polymerization of BPDA and DMB in *p*-chlorophenol. BPDA–DMB having a monomer concentration of 10% (w/w) remained completely in solution during polymerization and the solution formed a gel at room temperature. The intrinsic viscosity of the BPDA–DMB in *p*-chlorophenol at 60 °C was 8–10 $dl\,g^{-1}$. BPDA–DMB fibres were produced in our fibre laboratory. The isotropic solutions of 10% (w/w) BPDA–DMB polymer in *p*-chlorophenol were used via a dry-jet wet spinning into a coagulation bath of water/acetone. The as-spun fibres were then drawn at an elevated temperature up to ten time draw ratio in air via a zone drawing method. Both the fibre spinning and zone drawing apparatus are schematically shown in Fig. 1 [4–7, 17].

2.2. Tensile recoil test

Kevlar-49 fibres having a diameter of 12 μm (Dupont Company) were selected as a reference material to quantitatively calibrate the instrument for fibre compressive strength measurements from the TRT method since the compressive strength of this fibre has been reported and widely accepted [13]. The test was carried out at 2.54 cm (one inch) gauge length. The kink band observations for Kevlar-49 fibres with respect to different stresses applied on the fibres are listed in Table II, and the results (N and K) are statistically treated via simple majority. It is clear that the compressive strength of this fibre is in the range of 365–375 MPa. This is in an excellent agreement with previously reported data [13].

BPDA-DMB fibres with different diameters ranging from 15–40 μm were prepared via controlling the spinneret diameters. These as-spun fibres underwent the same draw ratio during annealing at an elevated temperature (425 °C) in order to achieve the same degree of crystallinity and orientation in these fibres since these factors may affect the fibre compressive strength. All the fibres tested were carefully examined in advance by polarized light microscopy (PLM, Olympus BH–2) in order to avoid possible pre-existing defects. The diameter of each fibre was individually determined via an accurate analysis (weight and size) to eliminate any non-uniformity of the fibres and decrease the experimental error. All the fibre samples were then mounted on the paper tabs by epoxy before the sample was gripped on a Rheometric solid analyser RSA II instrument. The paper tabs had a gauge

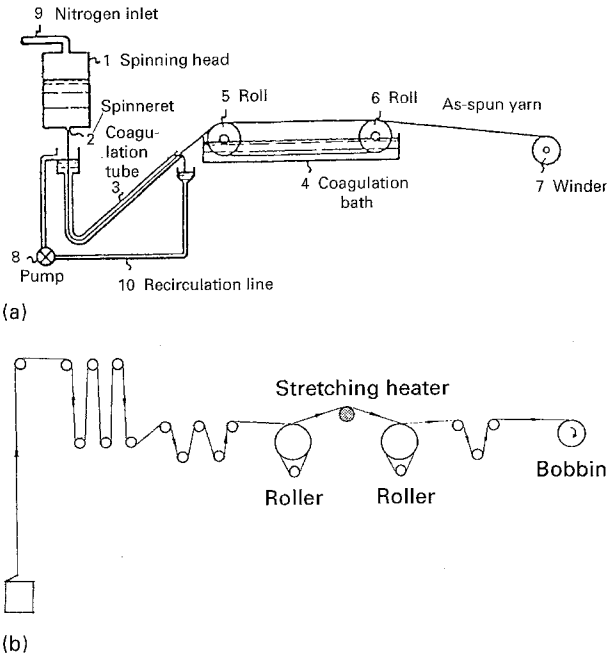

Figure 1 Schematic drawing of (a) the dry-jet wet spinning [17] and (b) the zone drawing and annealing set-up. (The rollers on the right revolve 10 times as fast as those on the left.)

TABLE II Tensile recoil test results in Kevlar-49 fibre*

Stress applied (MPa)	Kink band observations**
330	N, N
330	N, N
340	N, N
350	N, N
350	N, K
360	N, K
360	N, K
370	N, K
370	K, K
380	K, K
380	K, K
390	K, K
400	K, K

*The fibre possessed a diameter of 12 μm, and the gauge length used was 2.54 cm.

**N is designated to indicate that no compressive damage observed; and K is designated to show that at least one kink band was observed. Pairs of the N and K represent the kink band observation of both the upper and lower parts of the fibre after fracture.

length of 2.54 cm and the strain rate was $1 \times 10^{-4}\,sec^{-1}$. The two arms of the paper tab were then cut off and the fibres were automatically stretched to a selected tensile load. After the fibre was ruptured using the electric spark and recoiled from the centre of the gauge length, the two parts of the fibre were removed from the instrument and the damage was examined at the grip ends using PLM. A series of tests were carried out at various levels of tensile load to obtain the minimum tensile stress required to damage (form kink bands) the fibre during recoil. This stress was taken as the axial compressive strength of the fibre. A change of the gauge length was carried out for three chemical-structurally similar aromatic polyimide fibres. Only minor gauge length dependence was found [18]. As a result, we choose the shortest gauge length of 2.54 cm as the standard in the TRT experiments for this study.

2.3. Compression experiments

All specimens were examined carefully via PLM to insure accurate fibre lengths and uniform diameters. Each single filament was embedded in a Nylon 6 (Mm = 20 000)–formic acid (88%) solution with minimum tension on a glass plate, very similar to the method reported previously [8]. Solutions having different concentrations of 3%, 5%, 10%, 15%, 20% and 25% (w/w) were used to form films, and placed on a hot plate isothermally kept at 55, 60, 65, 70, 75 and 80 °C correspondingly. The thickness of good quality films ranged from 30–50 μm depending on the concentration of the solution and coating processes. During the evaporation of formic acid in the films, the matrix nylon 6 shrinks to form a uniform compressive force field around the fibre. The films formed on the glass plates were removed by using a sharp razor and the compressed fibres were isolated via dissolving the nylon 6 matrix in formic acid at room temperature. The fibres were then water-washed 3–4 times and dried in a vacuum oven at 105 °C for 2 h. These single filaments were examined again under PLM to obtain the fibre lengths after compression. Non-uniformly compressed fibres were excluded in this examination.

2.4. Tensile property measurements

Both single filaments before and after compression were carefully mounted on paper tabs with epoxy and the filament was clamped onto a Rheometric RSA II for tensile property measurements. The gauge length was chosen to be 2.54 cm and the strain rate was $1 \times 10^{-4}\,sec^{-1}$. Tensile stress–strain curves were obtained for both filaments under the same test conditions.

2.5. Fibre morphological observations

The kink band textures on the fibre surfaces of the pre-compressed fibres were observed using a PLM and scanning electron microscopy (SEM, JSM-U3). These experiments provided the kink band size, the angle of the kink bands with respect to the fibre axis, and the kink band density with the change of compressive strain. For the SEM observations, the initiation of the kink band was also investigated. The skin-core texture was observed via a fibre peeling technique.

2.6. Dynamic mechanical analysis

Possible relaxation processes were examined via the Rheometrics RSA II and a Seiko DMS 200 from − 130–550 °C. A multiple frequency sweeping mode was utilized between 0.1–10 Hz. The displacement was 0.01%, and gauge length was 2.54 cm. Special care was taken regarding the perfect alignment of the fibres on the sample clamps in order to obtain reproducible results. An apparent relaxation strength was calculated based on the integration of the intensity of tanδ with respect to reciprocal temperature [19] under the assumption that the relationship between frequency and temperature obeys the Arrhenius

equation. Activation energies of the subglass relaxations were also calculated via the peak temperatures of E″ based on this equation.

3. Results and discussion

3.1. Compressive strength of the BPDA–DMB fibres

For BPDA–DMB fibres, Tables III and IV illustrate detailed results of the kink band observations for two different fibre diameters measured via the TRT method. The compressive strengths obtained in fibre diameters ranging between 15–40 μm are shown in Fig. 2. As described previously, these BPDA–DMB fibres were carefully prepared via controlling processing conditions, and possess the same crystallinity (around 65–70% at a draw ratio of ten), degrees of the crystal orientation (around 90%), and overall orientation (around the birefringence of 0.25–0.26). From our experimental observations, the effect of diameter on compressive strength does not seem to be significant in this range. For example, at a diameter of 22.4 μm, the compressive strength is 655 MPa, and it is slightly increased to 675 MPa when the diameter increases to 40.6 μm. A similar observation in PBZO was reported a few years ago. In a diameter range between 25–75 μm, no significant change of the compressive strength of the fibres was found [1].

TABLE III Tensile recoil test results for BPDA–DMB fibres with gauge length of 2.54 cm and a diameter of 22.8 μm

Stress applied (MPa)	Kink band observations
600	N, N
600	N, N
620	N, N
630	N, N
640	N, N
640	N, K
650	N, K
655	N, K
660	N, K
660	K, K
670	K, K
690	K, K

TABLE IV Tensile recoil test results for BPDA–DMB fibre with a gauge length of 2.54 cm and a diameter of 39.6 μm

Stress applied (MPa)	Kink band observations
700	N, N
710	N, N
720	N, N
730	N, N
740	N, N
740	N, N
750	N, N
750	N, K
760	N, K
770	N, K
780	N, K
790	N, K
800	K, K

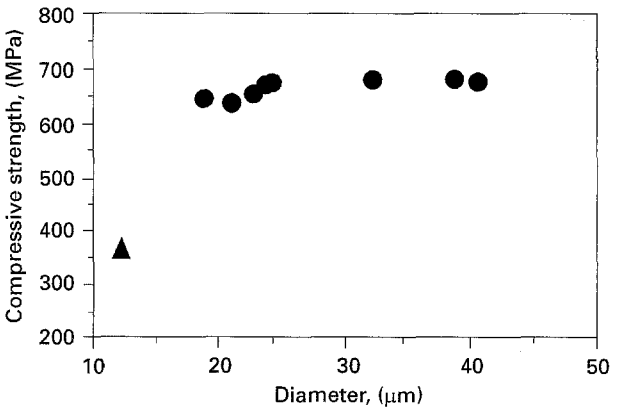

Figure 2 Relationship between the compressive strength measured via TRT and fibre diameters for (●) BPDA–DMB fibres and (▲) Kevlar-49 fibre.

In Kevlar fibres, the change of the gauge length in the TRT method does not significantly affect the determination of the compressive strength [13]. However, it has also been reported that Asahi-A5 fibres show a significant increase of the compressive strength with a gauge length between 2–8 cm [13]. For the TRT experiments in BPDA–DMB fibres, the gauge length of 2.54 cm was used. Generally speaking, if a fibre shows viscoelastic behaviour, a longer gauge length may introduce more energy dissipation through that behaviour prior to the kink band formation compared to the case having a shorter gauge length. However, even if the compressive strength of BPDA–DMB fibres is slightly dependent on the gauge length [18], our measured value should represent a value close to the lowest one and close to the extrapolated value at zero gauge length since the shortest gauge length was used. As a result, we conclude that BPDA–DMB fibres do exhibit a higher compressive strength compared with other high-performance polymeric fibres.

The critical compressive strain, ε_c, can be determined via the matrix shrinkage technique using nylon 6-formic acid solution at different concentrations. The observations of kink band formation have been carried out through PLM and SEM. A critical compressive strain of 0.51–0.54% has been found based on the observation of permanent kink band appearance (see below). These data were statistically averaged in fifty independent experimental observations at each applied compressive strain. It should be noted that for different fibres, the critical strain at which the first appearance of the kink band is observed is different due to variations in fibre structure and morphology [20, 21]. For example, PBZT and PBZO fibres do not show kink bands until the compressive strain is up to 0.1% based on optical microscopic observations [22–24], while for the Kevlar fibres the critical compressive strain has been reported to be between 0.3–0.5% [9, 23, 24]. Although this critical strain may vary depending upon the different measurement methods, the critical compressive strain for BPDA–DMB fibres is relatively higher when compared to other high performance fibres, indicating that this fibre is able to dissipate energy more efficiently

than other high performance polymeric fibres. As a result, the kink band formation, which is the final resort for the energy dissipation, occurs even at the higher compressive strain. This ε_c value should represent the upper limit for the critical compressive strain of the kink band formation.

The origin of this high compressive strength for BPDA–DMB fibres may be attributed to many aspects. One of the aspects may be associated with the fibres' viscoelastic behaviour since after all the crystallinity is only about 65–70% in the fibres. This can be investigated by using the apparent relaxation strength which has been defined in the experimental section via DM experiments. Fig. 3 shows the relationship between the intensities of tanδ and temperature for BPDA–DMB fibres at different draw ratios in the temperature range between −130–500 °C at 1 Hz. The data for Kevlar-49 fibres is also included and used as a normalizing factor. It is clear that at about − 30 °C a subglass relaxation (γ relaxation) can be found in BPDA–DMB fibres. The activation energy obtained via the Arrhenius equation is 150 kJ mol^{-1} for as-spun fibres, and it increases to 184 kJ mol^{-1} for the fibres after drawing ten times. Above room temperature, the β relaxation occurs at around 140 °C. An activation energy of 160 kJ mol^{-1} and 210 kJ mol^{-1} for the as-spun and the ten-time drawn fibres, respectively. An α relaxation occurs above 330 °C which is the glass transition [6]. All three relaxation processes show serious draw ratio dependence and, therefore, a crystallinity and orientation dependence [6]. Of major importance in this study is the fact that the apparent relaxation strength of the BPDA–DMB fibre decreases with increasing the draw ratio as shown in Fig. 4. The values of the apparent relaxation strength of BPDA–DMB fibres in this figure are the ratios between the integrations of the fibres at each draw ratio and that of Kevlar-49 fibres. Even at a draw ratio of ten, the apparent relaxation strength of this fibre is still 2.5 times higher than that of Kevlar fibres. Note that in the case of BPDA–DMB fibres having a draw ratio of ten, they have exhibited equivalent tensile strength and modulus compared to Kevlar -49 fibres. The higher apparent relaxation strength is thus

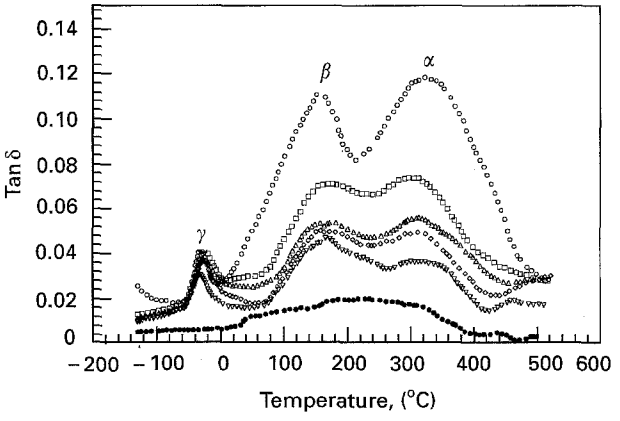

Figure 3 Relationships between tanδ and temperature for BPDA-DMB fibres with different draw ratios of; (○) As spun, (□) 3×, (△) 5×, (◇) 7×, (▽) 10× and (●) Kevlar-49 fibre via DM measurements.

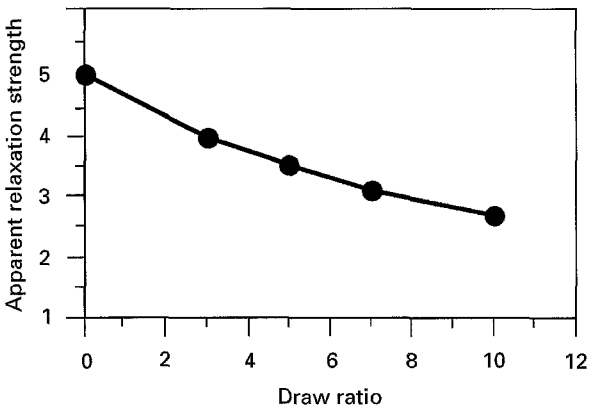

Figure 4 Relationship between the apparent relaxation strength and draw ratio in BPDA–DMB fibres.

an indication of high energy absorption and dissipation. Therefore, the energy transfer along the BPDA–DMB fibre after the fibre was ruptured in TRT experiments may not be as efficient as that in PBZT, PBZO and Kevlar-49 fibres. Some of the energy may be spent to stimulate molecular motion in subglass relaxations particularly in the γ relaxation of the fibres. The energy used to form kink bands in BPDA–DMB fibres is thus also less effective compared to those other fibres.

3.2. Morphological observations of the compressed fibres

As expected, BPDA–DMB fibres exhibit kink band formation as a result of compressive failure similar to the other high performance polymer fibres. Figs 5–8 illustrate the fibre morphology of BPDA–DMB fibres at various compressive strains. At a compressive strain of 0.70%, which is slightly above the critical compressive strain (0.51–0.54%), an initiation of the kink band formation can be recognized and it is marked by an arrow in Fig. 5. Note that only at the right side of the fibre does a kink band appear. This type of morphology may be an indication of a kink band nucleation process. With increasing the compressive strains to 1.2%, the compressive damage can be found to cross over the whole filament (Fig. 6), representing a growth of the kink band. The size of the kink band along the fibre direction is rather small (about 0.05–0.1 μm) with sharp boundaries between the kink band and unkinked regions. Further increases in the compressive strain to 2.3% show that a large scale kink formation has been formed, and the size of the kink band along the fibre direction is several micrometers as shown in Fig. 7. The cracks, both parallel and perpendicular to the fibre directions, are also evident. This indicates that permanent damage to the fibre structural integrity due to the compressive failure is inevitable. These observations of kink bands are similar to those reported in Kevlar, PBZT and PBZO fibres [13, 25, 26]. When the compressive strain excesses 3%, a large scale *S*-shaped buckling kink is observed as shown in Fig. 8. This reveals that the compression is no longer uniformly applied at every kink band along the fibre but that the deformation occurs at the weakest, least

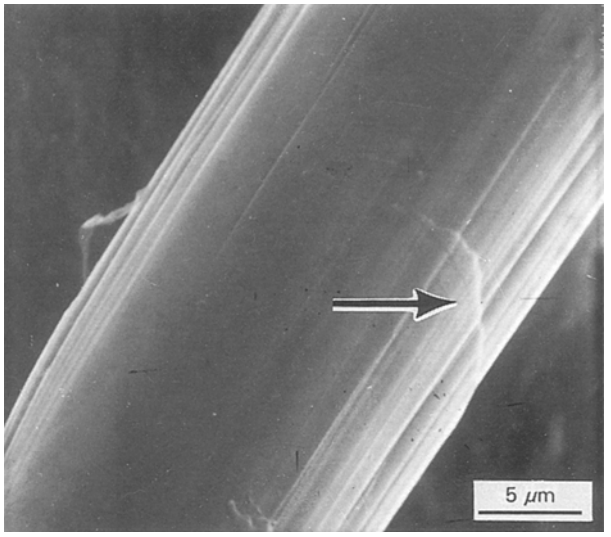

Figure 5 SEM micrograph for a pre-compressed fibre at a strain of 0.78%. A kink band has been initiated on the fibre surface at the right side pointed out by an arrow.

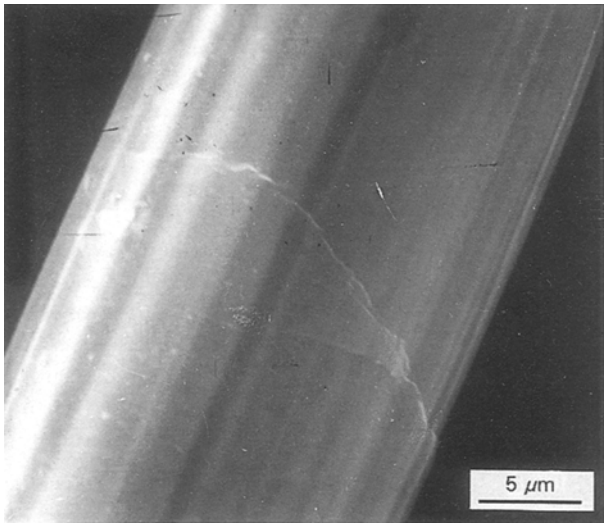

Figure 6 SEM micrograph of a kink band formed on a pre-compressed fibre at a strain of 1.2%.

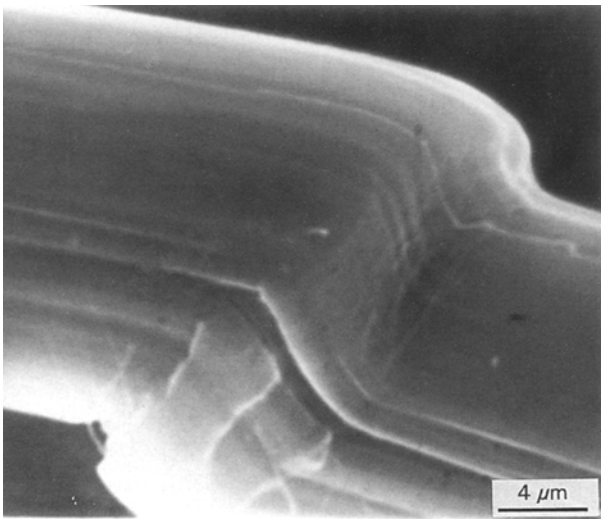

Figure 7 SEM micrograph of a kink band formed on a pre-compressed fibre at a strain of 2.3%.

stable position along the fibre tested due to the stress concentration there. Apparently, each kink band itself can no longer dissipate all the energy generated during the compression. This is the second critical compressive strain at which the large scale deformation takes place.

From PLM observations on the matrix compressed BPDA–DMB fibres, it is clear that the kink band always forms at an angle of $\pm 60°$ ($\pm 2°$) with respect to the fibre axis (Fig. 9). The direction of the kink band

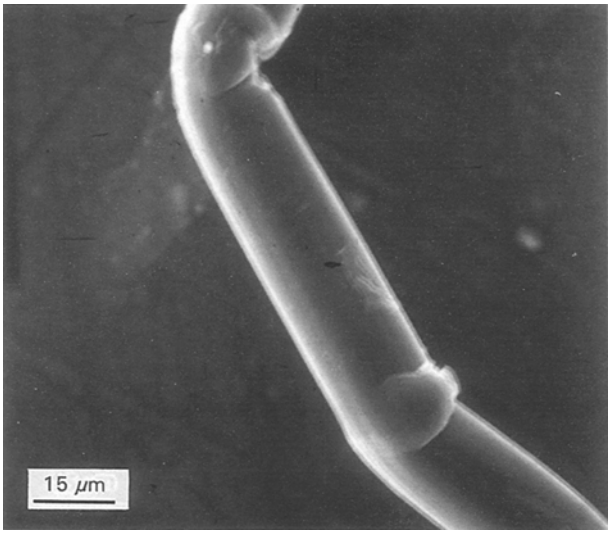

Figure 8 SEM micrograph of a kink band formed on a pre-compressed fibre at a strain of 3.2%.

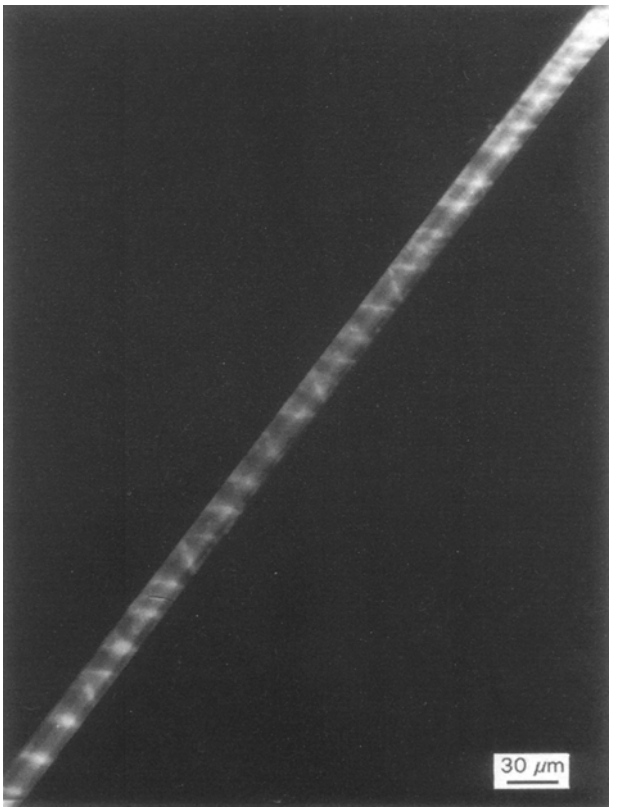

Figure 9 PLM observations of the kink band texture, and that the angle between the kink band and the fibre axis is around ± 60 (± 2)°. In some locations V-shaped bands can also be observed.

(negative or positive) is more or less random. In some locations, a *V*-shaped band is observed, which consists of two neighbouring kink bands with opposite directions to the fibre (+ 60° and − 60°, respectively). It has been reported that the kink band angle is closely related to the fibre structure and properties [20, 21]. In annealed PBZO fibres, the angle is around ± 67° [23], while for Kevlar fibres, it is between ± 50 − ± 60°. In BPDA–DMB fibres crystallite sizes are rather small and the crystallinity is about 65–70% [6, 26]. The kink bands may be initiated within a highly oriented non-crystalline region or within the crystals. Furthermore, it is interesting to note that the triclinic unit cell of BPDA–DMB crystals possesses an angle of $\alpha = 61.2°$ [6, 27]. Detailed structural analysis for the possible kink band formation via the slippage mechanism is in progress. It should also be cautioned that using PLM to observe the kink band angle may not clearly distinguish individual kinks due to the limited resolution but rather shows a contribution through a bundle of kink bands [24–26]. Furthermore, only in the correct position (in-plane position) would one obtain the correct angle.

With increasing the compressive strain to about 1%, the kink band density drastically increases from zero to above 50 per mm (note that the critical compressive strain is between 0.51–0.54%). At the compressive strain of around 1.1%, the kink band density is at its maximum. A further increase of the compressive strain leads to a surprising decrease of this density, and at around 2%, it reaches about 15–20 per mm. Finally, the kink band density seems to be stabilized under further compression. These results are shown in Fig. 10. In PBZO fibres, a continuous increase of the kink band density with compressive strain has been reported up to slightly higher than ε_c, while in Kevlar fibres this density first increases and then reaches a plateau when further increases in the strain exceeded ε_c [23]. The explanation of the increase of the kink band density below 1% compressive strain seems to be clear and logical. In this strain range, the kink bands are uniformly initiated (nucleated) after the critical compressive strain is reached, and each kink band (bundle) may absorb approximately an equal amount of energy during the growth. After the maximum at above 1.1%, the decrease of kink band density may be the cause of a merger of neighbouring kink bands (bundles) due to the growth of individual kink bands in size along the fibre direction. Fig. 11 clearly shows the change of the kink band density with increasing the compressive strain (from 0.72–2.5%). Above a strain of 3.0%, the second critical compressive strain is reached, and the large scale, *S*-shaped buckling kink occurs to form a buckled link-hinger shape [28]. No quantitative data for the number of kink bands can be obtained.

Finally, it is also important that BPDA–DMB fibres possess a skin–core structure and microfibrillar texture, similar to other polymer fibres. This can be clearly seen from SEM observations as is shown in Fig. 12 for a fibre which was peeled apart from the centre along the fibre direction. The skin layer of this fibre is very thin and is on the order of ten to 30–50 nm. In the centre of the fibre, the microfibrillar texture has a submicrometer diameter and a length of a few micrometers. Sometimes, the microfibrilles can be observed to have a sheet-like shape [27]. The reason for the formation of this kind of microfibrillar texture must be closely associated with the fibre processing conditions. However, detailed relationships are not clear at this moment. Furthermore, at the corner of the peeled half fibre, buckling on the fibre

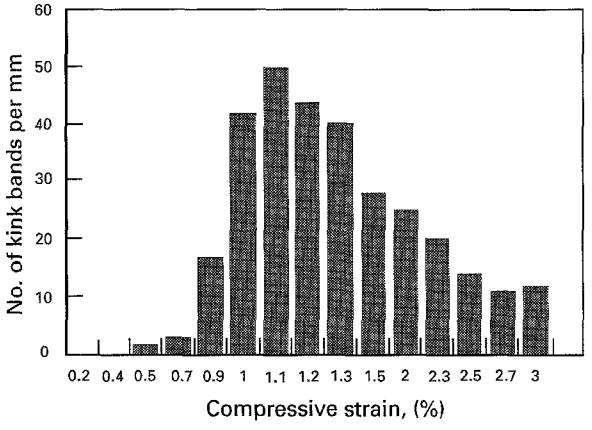

Figure 10 Relationship between the kink band density and the compressive strain for BPDA–DMB fibres of a diameter of 29.8 μm and a draw ratio of 10×.

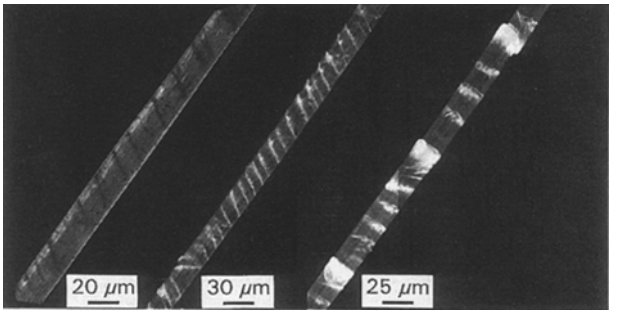

Figure 11 PLM microphotographs of the kink band formation at three different compressive strains (0.7%, 1.2% and 2.3% from left to right).

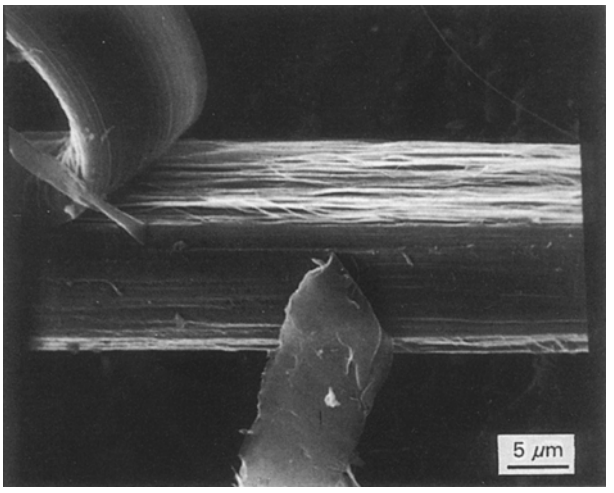

Figure 12 SEM observation of the skin–core structure and microfibrillar texture in a peeled fibre.

surface is evident. This reveals that in a large scale shear stress field (due to the peeling), a compressive banding deformation can be formed.

3.3. Tensile properties of pre-compressed fibres

The stress–strain curves of before and after compressed BPDA–DMB fibres with different degress of compressive strains are shown in Fig. 13. The tensile properties of BPDA–DMB fibres before and after compression are listed in Table V. It is interesting that the pre-compressed fibres show a progressive loss in initial tensile strength with increasing the compressive strain. This is because the initial tensile stress is spent to unfold the kink bands of the BPDA–DMB fibres. As soon as the kink bands are stretched out, a modulus similar to the normal fibres without compression can again be obtained. However, a substantial loss of the fracture energy is observed, and this loss increases with the compressive strain (Table V). Considering the skin–core structure in the fibres, the observations of the low initial modulus of pre-compressed fibres and the recovered high stiffness of unfolded fibres, one may conclude that the kink band occurs throughout the whole fibre cross-section rather than on the fibre surface alone.

Furthermore, the loss in tensile strength implies that the BPDA–DMB fibre with rigid-rod structure possesses weak interactions between microfibrilles. High-temperature fibres are usually formed through extended chain conformation and relatively rigid chain molecules. This is provided that the covalent bonding direction is along the fibre axis and only van der Waals interactions remaining in the transverse direction. An ordered crystal structure with high chain and crystal orientation often does not provide a large degree of freedom for accommodating an axial compression without any permanent structure damage. On the other hand, a 10–30% loss of the tensile strength shown in Fig. 13 seems unlikely to be attributed to an occurrence of a large degree of chain scission. Instead, chain slippage to form concentrated defect regions may be responsible for this decrease. A similar observation has also been reported in the case of Kevlar-49 fibres [8].

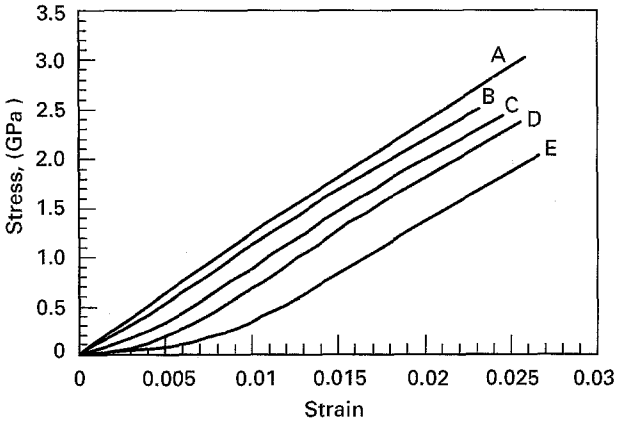

Figure 13 Stress–strain tensile relationships of the pre-compressed fibres at different strains. (A) as received (29.8 μm), (B) 1%, (C) 1.5% (D) 2% and (E) 3%.

4. Conclusions

The BPDA–DMB fibres have a compressive strength of 665 ± 5 MPa which is much higher than that of Kevlar-49 (365 MPa), PBZT (275 MPa) and PBO fibres (200 MPa). The effect of the diameter on the compressive strength of this fibre is not significant in a fibre diameter range between 15–40 μm. The relaxation processes may serve as one of the factors which significantly affect the compressive strength of BPDA–DMB fibres as evidenced by its high relaxation strength. PLM and SEM observations show that BPDA–DMB fibres form kink bands at ± 60 (± 2)° to the fibre axis during the compression, which start at a compressive strain of 0.51–0.54% (the critical compressive strain). With increasing the compressive strain, the kink band density increases first up to about 1.1% (50 per mm). Further increasing the strain leads to a decrease of the kink band density (15–20 per mm) due to the merging of neighbouring kink bands. Tensile tests of previously-compressed fibres revealed a 10–30% loss in tensile strength after the application of as much as a 2.6% compressive strain. The observations of the existence of a microfibrillar texture in BPDA–DMB fibres also indicate that BPDA–DMB fibres are similar to other polymer fibres with relatively weak transverse interactions.

Acknowledgement

This work was supported by the NSF Centre for Molecular and Microstructure of Composites (CMMC) and SZDC's Presidential Young Investigator Award from the National Science Foundation (DMR-9157738). Helpful discussion and information from Dr S. Allen at Dupont and Professor D. C. Martin at University of Michigan are also gratefully acknowledged.

TABLE V Tensile properties of compressed BPDA–DMB fibre

Compression (%)	Strength (GPa)	Strain (%)	Modulus (GPa)	Fracture energy (MPa)
0.0	3.0	2.6	135	38.8
1.0	2.55	2.3	135	29.4
1.5	2.45	2.5	134	28.8
2.0	2.39	2.6	134	26.3
2.6	2.08	2.7	135	21.6

References

1. S. KUMAR and T. E. HELMINIAK, in "*The Materials Science and Engineering of Rigid-Rod Polymers*", Materials Research Society Symposium Proceeding, edited by W. W. Adams, R. K. Eby and D. E. McLemore, Vol. 134 (1989) pp. 363–374.
2. M. G. DOBB, D. J. JOHNSON and B. P. SAVILLE, *Polymer* **22** (1981) 960.
3. J. M. GREENWOOD and P. G. ROSE, *J. Mater. Sci.* **9** (1974) 1809.
4. S. Z. D. CHENG, Z. WU, M. EASHOO, S. HSU and F. W. HARRIS, *Polymer* **32** (1991) 1803.
5. M. EASHOO, Z. WU, D. SHEN, S. HSU, C. J. LEE, F. W. HARRIS and S. Z. D. CHENG, *ibid.* **34** (1993) 3209.
6. M. EASHOO, D. SHEN, Z. WU, C. WU, F. W. HARRIS, S. Z. D. CHENG, K. GARDNER and B. S. HSIAO, *Macromol. Chem. Phys.* **195** (1994) 2207.
7. D. SHEN, Z. WU, S. LEE, F. W. HARRIS, S. Z. D. CHENG, J. BLACKWELL, T. WU and S. CHVALUN, *Polymers and Polymer Composites* (in press).
8. S. J. DETERESA, R. J. FARRIS and R. S. PORTER, *Polym. Comps.* **3** (1982) 57.
9. S. J. DETERESA, S. R. ALLEN, R. J. FARRIS and R. S. PORTER, *J. Mater. Sci.* **19** (1984) 57.
10. S. J. DETERESA, R. S. PORTER and R. J. FARRIS, *ibid.* **23** (1988) 1886.
11. D. SINCLAIR, *J. Appl. Phys.* **21** (1950) 380.
12. L. T. DRZAL, AFWAL-TR-86-4003.
13. S. R. ALLEN, *J. Mater. Sci.* **22** (1987) 853.
14. S. A. FAWAZ, A. N. PALAZOTTO and C. S. WANG, *Polymer* **33** (1992) 100.
15. K. S. MACTURK, R. K. EBY and W. W. ADAMS, *ibid.* **32** (1991) 1782.
16. C. S. WANG, S. J. BAI and B. P. RICE, in Proceedings of Polymeric Materials Science and Engineering, (ACS, Washington D.C. 1989) **61** 550.
17. H. H. YOUNG, "Aromatic High Strength Fibres", (Wiley & Sons, New York, 1989) p. 758.
18. Unpublished work.
19. I. M. WORD, "Mechanical Properties in Polymers", (Wiley Interscience, New York, 1971) Ch. 5.
20. S. VAN DER ZWAAG and G. KAMPSCHOER, in "Integration of Fundamental Polymer Science and Technology", 2nd edn. (Elsevier, London, 1988) Ch. 2, p. 545.
21. S. VAN DER ZWAAG, S. J. PICKEN and C. P. VAN SLUIJS, in "Integration of Fundamental Polymer Science and Technology", 2nd edn. (Elsevier, London, 1989) Vol. 3, p. 199.
22. W. HUH, S. KUMAR, T. E. HELMINIAK and W. W. ADAMS, *SPE Annual Tech. Conf. Proc.* (1990) 1245.
23. D. C. MARTIN and E. L. THOMAS, in Pre-print of 8th International Conference of Deformation, Yield and Fracture of Polymers, Churchill College, Cambridge, UK.
24. D. C. MARTIN, Ph.D dissertation, Department of Polymer Science and Engineering, University of Massachusetts, Amherst, MA, 1990.
25. D. C. MARTIN and E. L. THOMAS, *J. Mater. Sci.* **26** (1991) 5171.
26. *Idem. Macromolecules* **24** (1991) 2224.
27. M. EASHOO, Ph.D. dissertation, Department of Polymer Science, University of Akron, Akron, OH, 1994.
28. S. J. DETERESA, R. S. PORTER and R. J. FARRIS, *J. Mater. Sci.* **20** (1985) 1645.

Received 7 July 1994
and accepted 1 December 1995